J Mater Sci: Mater Med (2011) 22:637–646
DOI 10.1007/s10856-011-4238-2

Hydroxyapatite-collagen composites. Part I: can the decrease of the interactions between the two components be a physicochemical component of osteoporosis in aged bone?

Niccoletta Barbani · Elisabetta Rosellini · Caterina Cristallini · Giulio D. Guerra · Adriano Krajewski · Mauro Mazzocchi

Received: 4 June 2010 / Accepted: 14 January 2011 / Published online: 30 January 2011

Abstract The interactions of Type I acid soluble collagen (Col) with both carbonate-free hydroxyapatite (HA_{1100}) and carbonate-rich one (CHA) were investigated. The aim was to ascertain whether the increase of bone CO_3^{2-} with ageing could relate to the disease known as osteoporosis. HA_{1100}-Col and CHA-Col composites with various ratios were prepared and examined. Scanning electron microscopy and differential scanning calorimetry showed a stronger adhesion of the Col matrix to the granules of HA_{1100} than to those of CHA. FT-IR spectroscopy showed that with HA_{1100} both multiple hydrogen bonds of Col peptide –NH groups with HA PO_4^{3-}, and electrochemical interactions between Col peptide –C=O groups and HA Ca^{2+} were present. In the presence of CO_3^{2-}, the interactions between –NH and phosphate were diminished, and Ca^{2+} interacted more strongly with CO_3^{2-} than with peptide –C=O, so causing a separation between the two components of the bone extra-cellular matrix. The results obtained strengthen the hypothesis that the substitution of PO_4^{3-} ions by CO_3^{2-} ions in the HA lattice might be a significant component of osteoporosis, although further investigation is needed.

N. Barbani · E. Rosellini
Dipartimento di Ingegneria Chimica, Chimica Industriale e Scienza dei Materiali, Università di Pisa, Largo Lucio Lazzarino, 56122 Pisa, Italy

C. Cristallini · G. D. Guerra (✉)
Istituto per i Materiali Compositi e Biomedici (IMCB), U.O.S. di Pisa, Consiglio Nazionale delle Ricerche (CNR), Largo Lucio Lazzarino, 56122 Pisa, Italy
e-mail: giuliodante.guerra@diccism.unipi.it

A. Krajewski · M. Mazzocchi
Istituto di Scienza e Tecnologia dei Materiali Ceramici (ISTEC), Consiglio Nazionale delle Ricerche (CNR), Via Granarolo 64, 48018 Faenza, RA, Italy

Present Address:
A. Krajewski
Ceramic Science and Technology, c/o Agenzia Polo Ceramico, Via Granarolo 62, 48018 Faenza, RA, Italy

1 Introduction

The extra-cellular matrix of the bone can be regarded as a composite between a fibrous protein matrix, mainly collagen (Col), and a mineral phase, mainly hydroxyapatite (HA), with lesser amounts of other calcium phosphates, calcium carbonate and other salts; the whole mineral phase, the amount of which varies with the age and the regions of the skeleton, is the most part of the composite [1]. A direct physical bonding between the collagen fibres and the apatite crystals has been ascertained in bone since more than 40 years [2], although recently the role of the osteopontin, a protein different from collagen, in the bone toughness [3], as well as in the tooth drift-associated bone remodelling [4], has been pointed out. During the ageing of the bone, some modifications in its structure occur, which with time result in the disease known as osteoporosis [5, 6]. The most relevant of them are the substitution of phosphate ions by carbonate ions in the HA lattice [7], a release of calcium due to metabolic acidosis [8], a general decrease of the bone mineral density [9], and some alterations of the cross-links between Col fibrils [10].

Considering the fact that, with ageing, an increase occurs of the CO_3^{2-} content in bone [7], mainly owing to the progressive diminishing of the respiratory effectiveness in eliminating CO_2 from blood, as well as to the pathologies involving HA and Col in bone, the authors decided to investigate whether these phenomena might be correlated.

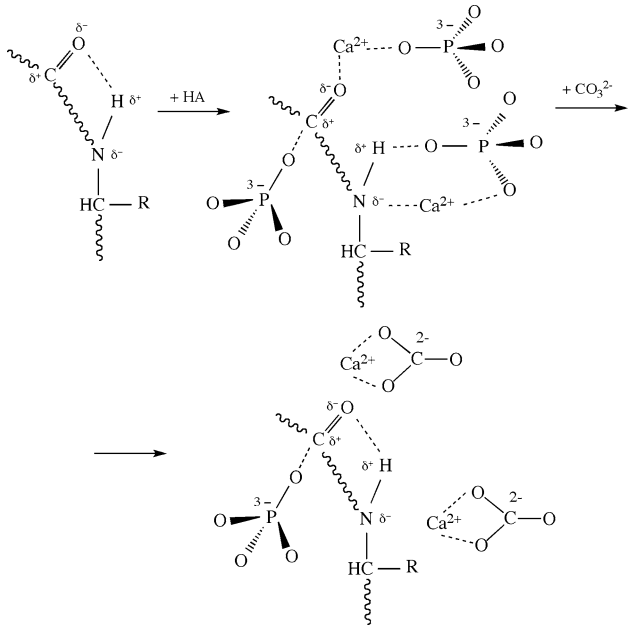

Fig. 1 Interactions between Col and HA both in the absence and in the presence of carbonate ions

The starting hypothesis was that the presence of CO_3^{2-} ions in the mineral phase could interfere with the ion–dipole interactions between the Ca^{2+} ions and the carbonyl groups present in the Col polypeptide chains (see Fig. 1). The hypothesis was tested with positive indications in previous works [11, 12].

The present paper reports an investigation of some physicochemical properties, carried out on Col-HA composites, both in the presence and in the absence of CO_3^{2-} in the mineral phase, with a particular attention to the interactions at the interface. A scheme of the main interactions is shown in Fig. 1; however, also the ionic interactions of the Ca^{2+} ions of HA with the carboxyl anions of the aspartic and glutamic acid units of Col must be taken into account; nevertheless, these interactions are less significant, because of the relatively low amount of these two amino acids: in the human skin, the Col α1 chain contains 4.1% aspartic acid and 7.1% glutamic acid, and the α2 chain contains 4.4% aspartic acid and 6.6% glutamic acid [13].

2 Experimental

2.1 Materials

Type I acid soluble Col (Sigma, Buchs, SG, Switzerland, from calf-skin) has a molecular weight of about 300 kDa.

Carbonate-free HA (HA_{1100}) was prepared in the ISTEC laboratories, following the standard procedure for a "biomedical grade" one [14], by a precipitation method, under continuous stirring, in a multi-neck Pyrex glass reactor, at a constant temperature of 85°C, under slow-flux N_2 atmosphere, dripping a H_3PO_4 solution in a $Ca(OH)_2$ suspension very slowly. To control continuously the pH variation, and in particular to monitor exactly the equivalence point for the theoretical chemical formula of HA, $Ca_5(PO_4)_3OH$, the pH-meter sensor was held constantly immersed in the suspension. The powder so obtained was dried in an oven at 90°C, and finally annealed at 1100°C for 1 h [15]. The carbonated HA (CHA, FinCeramica Faenza, Italy, lot n. 0401160002, declared carbonate molar percentage 14.5%) was used as supplied. The elemental analysis ascertained that the actual content of CO_3^{2-} in the lattice of CHA was 16.5 ± 1.5%. Conversely, the same analytical technique did not detect any CO_3^{2-} in HA_{1100}, which was found to have the composition of a stoichiometric one [11, 15]. A carbonate-free HA and a greatly carbonated one were used, in order to investigate either the maximum or the minimum possibility of physicochemical interactions between HA and Col. Both powders were milled into almost spherical granules, using a jar mill with ZrO_2 balls as grinders, then sieved to obtain powders with a mean diameter ranging between 30 and 60 μm.

The Col-HA composites were prepared by the following procedure. A 0.6% w/v Col solution was made dissolving the protein in 0.5 M acetic acid under continuous stirring in ice bath for 5 h. Two series of composites were prepared adding to the solution either HA_{1100} or CHA, in different weight ratios, under stirring for 5–10 min at room temperature. The HA to Col weight ratios in each series were the following: 10:90, 30:70, 50:50, 80:20. The ratios up to 50:50 were chosen because it was found that they were the most suitable to ascertain how the properties of the composites vary with the increasing HA content [11]; the 80:20 ratio, besides being very close to that present in the natural bone, is that of a nanocomposite, which was tested successfully on dogs [16]. The materials were manufactured as thin films, by drying the suspensions under ventilated hood at room temperature for about 48 h.

2.2 Analytical techniques

The elemental analysis of the carbon, used to calculate the amounts of carbonate present in both HA_{1100} and CHA, was performed by means of an elemental automatic analyser (Finnigan Flash EA 1112, with TCD detector, Finnigan, Bremen, Germany), equipped with a mass spectrometer, using Na_2CO_3 powder as a reference standard. The oxidation tube was kept at 1000°C, the reduction one at 680°C.

The scanning electron microscopy (SEM) was carried out by means of a JEOL (Pieve Emanuele, MI, Italy) T-300

instrument, on samples coated with 24 carat gold in a vacuum chamber.

Differential scanning calorimetry (DSC) was carried out in triplicate with a Perkin Elmer (Norwalk, CT, USA) DSC7 apparatus in hermetic steel pans from 10.00 to 100.00°C at 10.00°C per min under N_2 flux. To perform the tests in the presence of excess H_2O, in each pan 10 µl of distilled water were added to the quantities of the composites containing 2.5 mg of Col each. So, the quantities of the materials tested by DSC were 2.5 mg of pure Col. 2.8 mg of each 10:90 composite, 3.6 mg of each 30:70 composite, 5.0 mg of each 50:50 composite and 12.5 mg of each 80:20 composite.

Total reflection and spotlight Fourier-transform infrared (FT-IR) spectra and maps were carried out by means of a Perkin Elmer Spectrum One FT-IR Spectrometer, equipped with a Perkin Elmer Universal ATR Sampling Accessory and a Perkin Elmer Spectrum Spotlight 300 FT-IR Imaging System, using the "image" mode of the instrument. For each sample, an area of 1 mm × 1 mm was defined to cover all the structures present in the composites, and an IR image was produced using a liquid nitrogen cooled, 16-pixel mercury cadmium telluride (MCT-A) line detector at a 25 µm per pixel resolution. An absorbance spectrum was recorded for each pixel in the µATR mode. We collected the spectra by touching the ATR objective on the sample and collected the spectrum generated from the surface layers of the sample. The spotlight software used for the acquisition was also used to pre-process the spectra. The spectral images were analyzed with a compare correlation image. The obtained correlation map indicates the areas of an image where the spectra were most similar to a reference spectrum. The spotlight software was also used to determine the ratio between areas related to absorption peaks of interest. Before capturing the IR image, the ZnSe window is measured as a reference, and a background spectrum was collected for each of the 16 pixels. All spectra were recorded in the mid infrared region (4000–750 cm^{-1}) at 16 scans/pixel; the spectral resolution was 4 cm^{-1}; the spatial resolution was 100 × 100 µm.

3 Results

In a preliminary study [11], it was found that the SEM micrographs of the fracture surfaces of both pure collagen and HA-Col composites show that the fibril structure of Col is present also in the composites up to 50:50 HA_{1100} to Col ratio, whereas the corresponding CHA-Col composites show a more disordered structure and a less evident fibril structure. As regarding the 80:20 composites, Fig. 2 shows that the composite containing HA_{1100} has a structure quite similar to that of the healthy bone, while Fig. 3 shows a whole structure very similar to that of an osteoporotic bone in that containing CHA.

The Col thermal behaviour has been investigated by means of the DSC, which can give information about the temperature of the denaturizing process (T_d) and then about the thermal stability of Col, i.e. the resistance of the protein molecule to unfold owing to the heat treatment. The thermal denaturation of Col samples causes the destruction of the triple helix and the unfolding of the separated single peptide strands into random coils. The first step of this helix-to-coil transition involves the disruption of the structural water hydrogen bonds bridging together the three chains of polypeptides forming the Col molecules; the second step involves the disruption of the hydrogen bonds between the helices of the α-chains. From the DSC curves it is possible to calculate also the specific enthalpy variation (ΔH) for the denaturation process. As shown in Fig. 4, only a significant endothermic event, attributable to the denaturation of Col, is present, in the temperature range between 10 and 100°C, in the DSC traces measured in the presence of excess water. The T_d and ΔH values are reported in Table 1 for both composite series. In the series of composites containing HA_{1100}, as the inorganic component percentage in the composite increases, the Col denaturation signal shifts quite regularly, from the value of 49°C of the 10:90 composite, a little lower than that of 54°C of the pure Col, towards higher temperatures, until to the 61°C of the 80:20 composite. Conversely, no analogous trend can be observed with CHA, where the values are very

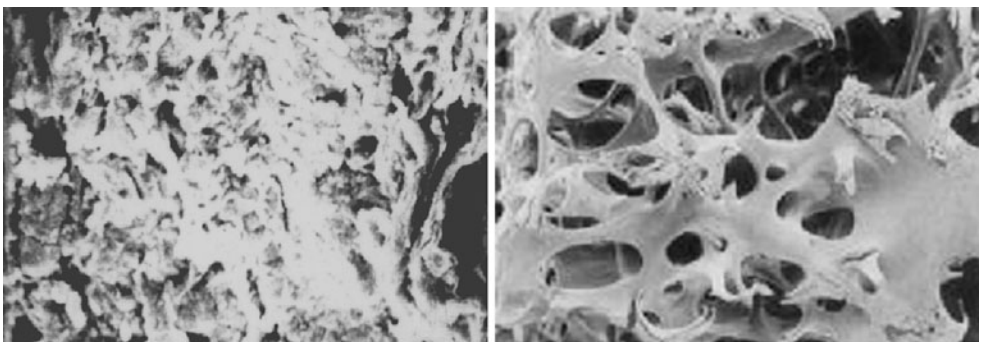

Fig. 2 SEM micrographs of the fracture surfaces of the 80:20 HA_{1100}-Col composite (*left*), and of a healthy bone (*right*) [1]

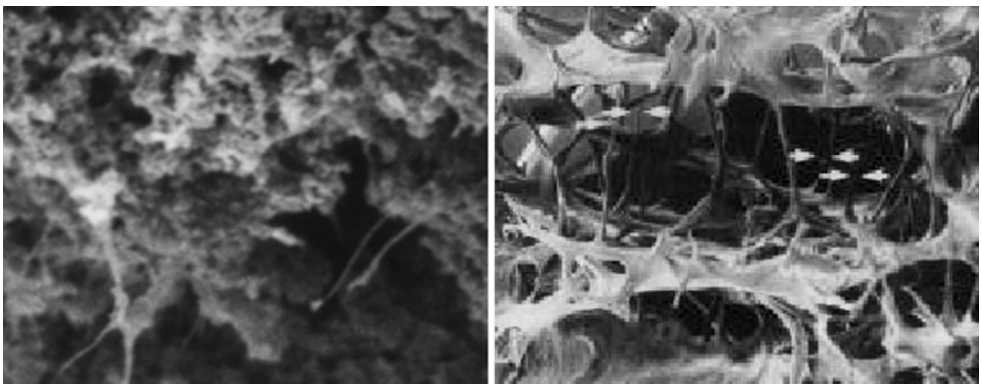

Fig. 3 SEM micrographs of the fracture surfaces of the 80:20 CHA-Col composite (*left*), and of an osteoporotic bone (*right*) [1]

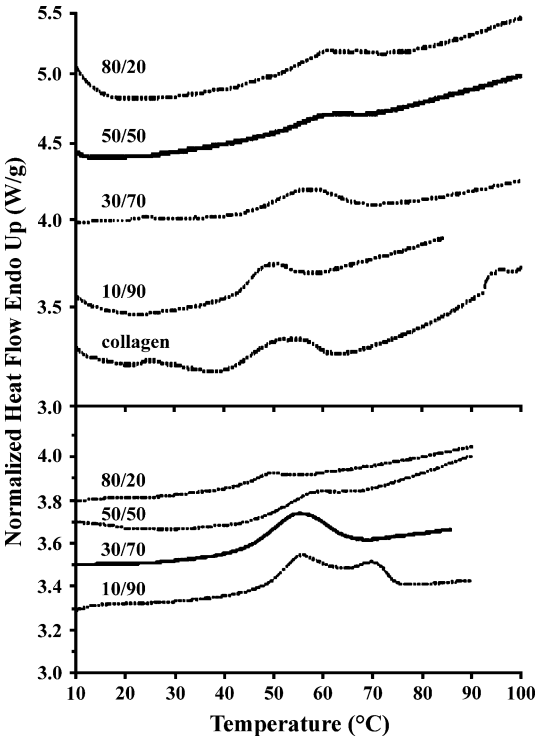

Fig. 4 DSC traces of: Col and HA_{1100}-Col composites (*upper graph*), and CHA-Col composites (*lower graph*), both having the signed hydroxyapatite to collagen ratios. The tests were carried out in hermetic steel pans, in the presence of 10 µl of added water. The heating rate was 10°C/min

similar to that of pure Col up to the 50:50 composite, while that of the 80:20 one falls to 49°C. At the same time, a splitting of the signal is seen in the trace of the 10:90 CHA-Col composite, with a second peak at 70°C, in addition to the main one at 56°C. As regarding the ΔH values, those of the composites containing HA_{1100} show a trend similar to the corresponding T_d values; also for the CHA-Col composites ΔH increases with decreasing the protein content, but all the values are lower than those of the HA_{1100}-Col ones.

Table 1 Temperatures of Col denaturation (T_d) and specific enthalpy variation (ΔH) for the pure Col and the composites of Col with both HA_{1100} and CHA, with different HA to Col ratios

HA:Col	HA_{1100}		CHA	
	T_d (°C)	ΔH (Jg^{-1})	T_d (°C)	ΔH (Jg^{-1})
0:100	54	16.7	54	16.7
10:90	49	14.6	56	12.6
30:70	56	14.8	54	13.2
50:50	60	15.1	58	14.4
80:20	61	20.1	49	16.8

Table 2 Most significant IR absorption bands of Col

Absorption band and related vibrations	Wave numbers (cm^{-1})
Amide I, due to the stretching of C=O	1635
Amide II, mainly due to the δN–H in plane, mixed with νC–N	1550
Amide III, mainly due to the νC–N, mixed with δN–H in plane	1240
νN–H sensible to hydrogen bond strength	3082–3342

Spotlight FT-IR Chemical Imaging Analysis gives useful information about the composite structure, and allows a very accurate investigation of the chemical composition of the material in different regions of the sample, giving transmission, total reflection and ATR spectra and images. The distribution of the components on the composite surface was analyzed by means of FT-IR Chemical Imaging. From the chemical map of each sample it was obtained the medium spectrum, in which it was possible to identify the typical bands of Col (see Table 2), as well as those of the phosphate anion at 812, 1041 and 1232 cm^{-1}. The correlation index between the chemical maps and the medium spectra was found to be close to the unit for the six composites examined (see Fig. 5). So, it was possible to

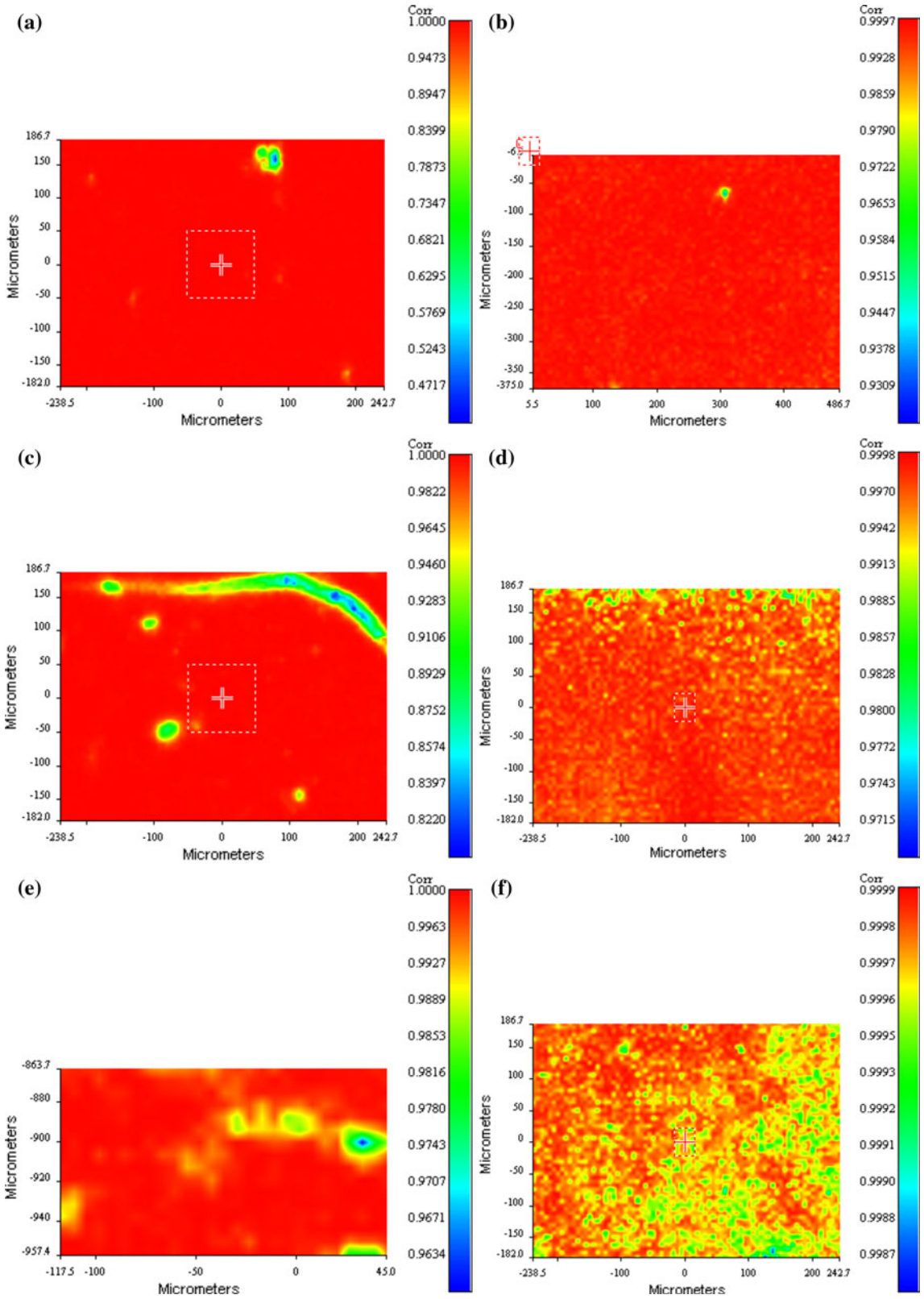

Fig. 5 Correlation maps for HA_{1100}-Col (*left column*) and CHA-Col (*right column*) composites, having the following HA to Col ratios: 10:90 (**a**, **b**); 30:70 (**c**, **d**); 80:20 (**e**, **f**)

Table 3 Ratios between the areas of the bands due to the protein matrix (amide I and amide II, from 1726 to 1487 cm^{-1}) and those due to the phosphate anion, between 1174 and 891 cm^{-1}. The values are the arithmetical means of the ratios between the areas measured in various regions of the maps

HA:Col	Ratios	
	HA_{1100}	CHA
30:70	1.32 ± 0.20	2.05 ± 0.05
50:50	0.48 ± 0.05	0.74 ± 0.05
80:20	0.30 ± 0.07	0.42 ± 0.07

ascertain a homogeneous distribution of the components on their surfaces, independently of the CO_3^{2-} content.

More information about the chemical homogeneity of the composites can be obtained from the ratios between the areas of the bands, taken in various regions of the maps, due to the protein matrix (amide I and amide II, from 1726 to 1487 cm^{-1}) and those due to the phosphate anion, between 1174 and 891 cm^{-1}. The data for the HA to Col ratios of 30:70, 50:50 and 80:20, reported in Table 3, indicate that the values did not vary very greatly within the maps and decreased with increasing the HA content in the composites, for both those with HA_{1100} and those with CHA, whereas all the latter were greater about 1.5-fold than the former.

The infrared absorption bands related to the Col groups able to undergo either electrostatic interactions with Ca^{2+} ions, like C=O, or hydrogen bonds with PO_4^{3-}, OH^- and CO_3^{2-} ions, like N–H, are listed in Table 2. The FT-IR analysis was then focused on the composites with a HA to Col ratio of 80:20, because it is both very similar to that present in the natural bone, and the most suitable to make bone reconstruction devices [16]. The aim of measuring the chemical interaction between the two components in the absence and in the presence of carbonate ions was to mimic the difference between healthy and osteoporotic bone. The ratio of the amide I absorbance areas to the amide II ones was evaluated, as well as the shift of their absorption frequencies, since these bands are sensitive to the structural changes within the Col molecules. Indeed, during the organization of Col into fibrils, the intensity of the amide II band increases greatly, owing to the lower hydration degree due to the substitution of H_2O molecules by HA crystals. Moreover, one can observe a shift towards lower frequencies of the amide I band at 1643 cm^{-1}, evident in the fibrils containing HA_{1100}, because the amide carbonyl stretching is weakened by the ion–dipole interaction with Ca^{2+}. Figure 6 shows spotlight FT-IR maps, measured on both Col-HA composites with a HA to Col ratio of 80:20. The chemical maps (Fig. 6a, c) show a quite uniform distribution of high-, middle- and low-absorbance areas in the maps for both composites. In Fig. 6b the ratio of the amide I band to the amide II one for the Col-HA_{1100} composite is shown: with few exceptions, the ratio ranges between values much lower and slightly greater than one. Conversely, the ratio between the amide I band and the amide II one for the Col-CHA composite (Fig. 6d) is greater than the unit in the most part of the map.

Figure 7 shows the spectra of both composites. The spectra of the Col-HA_{1100} composite, taken in the areas having the signed amide I to amide II band ratios, are shown in Fig. 7a–c. The spectra of the composite containing CHA instead of HA_{1100}, taken at the ratios of 1.00 and 1.30, are shown in Fig. 7d and e.

Figure 8a shows the absorbance spectra of the 80:20 HA_{1100}-Col composite, measured in the wave number interval between 1800 and 1200 cm^{-1}, taken at the points having amide I to amide II band ratios (R) equal to 1.40, 1.00 and 0.77, respectively. The comparison shows a shift, with decreasing R, of the amide I peak towards lower wave numbers and of the amide II one towards higher wave numbers, namely 1552 cm^{-1} for R = 1.40, 1559 cm^{-1} for R = 1.00 and 1570 cm^{-1} for R = 0.77. This effect, together with the decreasing of the absorbance greater for amide I than for amide II, causes the amide I band to appear as a shoulder of the amide II one in the spectrum taken at the lowest R. The analogous comparison between the spectra of the 80:20 CHA-Col composite (see Fig. 8b), taken at the R values of 1.40 and 1.00, shows only, in the spectrum at R = 1.00, a flattening of the amide I band and a shift of the amide II maximum from 1552 to 1565 cm^{-1}.

4 Discussion

All the experimental results show significant differences between the composites containing HA_{1100} and those containing CHA. However, the differences are not due to the distribution of the inorganic component within the Col matrix. Indeed, the quite constant correlation values, shown by the FT-IR correlation maps in Fig. 5, indicate the same substantially uniform distribution of both the HA_{1100} granules and the CHA ones within the Col matrix. Also the microanalysis spectra, carried out previously [11], confirmed that there is no significant difference in the distribution of both apatites within the whole collagen matrix. As regarding the morphological analysis made by means of SEM, the most significant results are the similarity of the 80:20 HA_{1100}-Col composite with the healthy bone (Fig. 2), and that of the 80:20 CHA-Col composite with the osteoporotic one (Fig. 3). The latter SEM image also resembles that of a composite formed with HA nanocrystals grown inside self-assembled collagen fibres [17].

The results of the thermal analysis, carried out by means of DSC, indicate that HA_{1100} is generally more effective

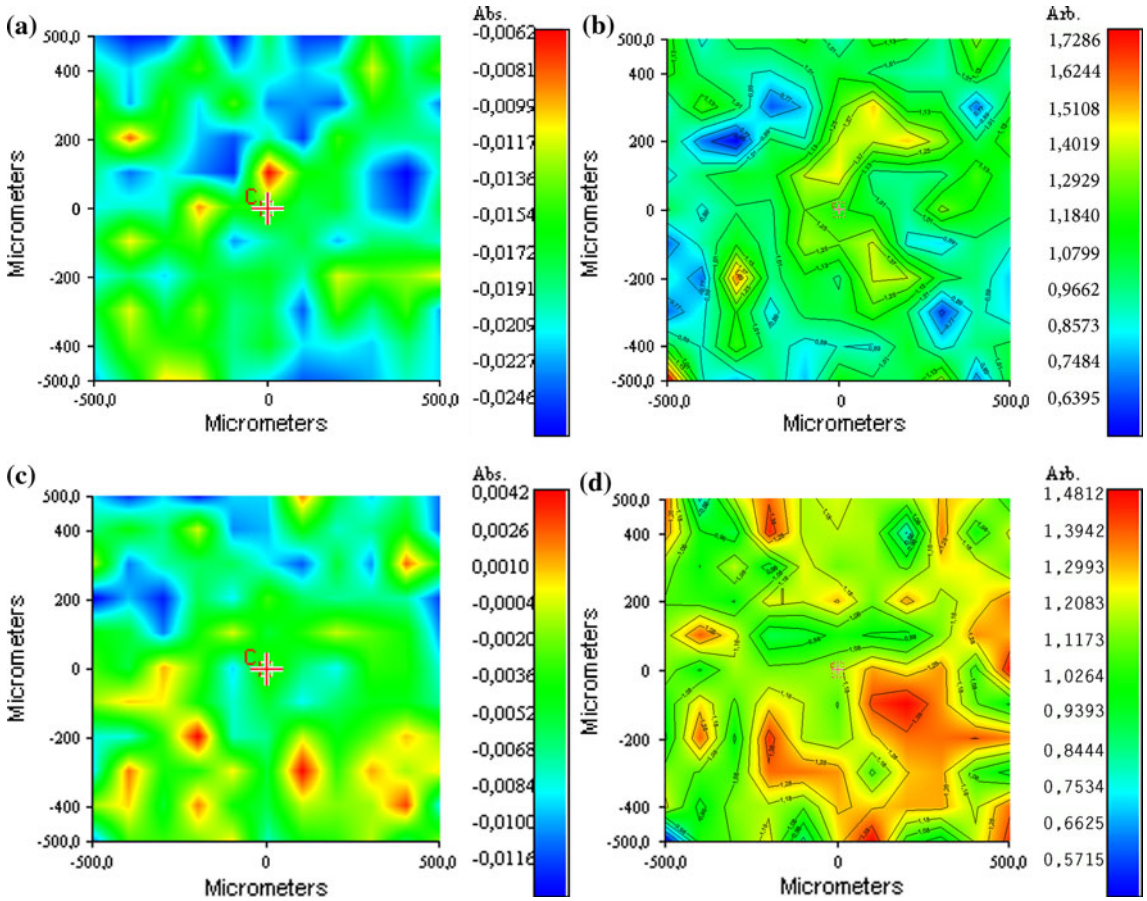

Fig. 6 Spotlight FT-IR maps of a HA_{1100}-Col 80:20 composite (*upper maps*) and of a CHA-Col 80:20 composite (*lower maps*). **a**, **c** Chemical maps; **b**, **d** amide I to amide II band ratios

than CHA in stabilizing the composite. The quite regular increasing of the T_d values in the upper graph of Fig. 4 and in the corresponding column of Table 1 indicates a stabilization of the protein structure by the inorganic filler in the HA_{1100}-Col composites, due to the presence of strong interactions between the two phases. This trend indicates also a diminishing of the presence of "bonded water" between the Col fibrils with increasing HA_{1100}, since part of the interacting water might be substituted by the HA crystals, which penetrates between the collagen fibrils. Conversely, the lower graph in Fig. 4 and the corresponding column in Table 1, where the T_d values show, up to the 50:50 CHA to Col ratio, a random trend and a close similarity with that of the pure Col, indicate that CHA cannot stabilize effectively the Col structure. As regarding the 80:20 composite, which has a composition quite similar to that of the natural bone, the Col structure seems even destabilized by CHA, since the strong lowering of its denaturation temperature, with respect to that of the pure protein (see Table 1). This fact can be explained with the presence of lower interactions between CHA and Col, which can interact more easily with water. As regarding the splitting of the Col denaturation signal in the trace of the 10:90 CHA-Col composite (see the lower graph of Fig. 4), it might be due to the presence of two different kinds of interaction, like those shown in Fig. 1. As regards the ΔH values, their trend, which is only a very qualitative one, is very similar for both series of composites. The only significant experimental data are the lower values, shown in Table 1, for the CHA-Col composites than for the HA_{1100}-Col ones: since the enthalpy variation is related to both the Col denaturation and the breaking of the ion–dipole links between the two phases of the composites, this lowering is an additional sign of the phase separation between the components of the bone structure, in the presence of a CO_3^{2-} excess, as a possible component of osteoporosis.

The correlation maps, shown in Fig. 5, indicate a substantially uniform distribution, in these composites, of both the HA_{1100} granules and the CHA ones within the Col matrix. Such distribution is confirmed by the ratios, reported in Table 3, between the areas of the bands, which differ quite little from each other when measured in different regions of the maps. As regarding the values observed for the CHA composites, greater than those of the

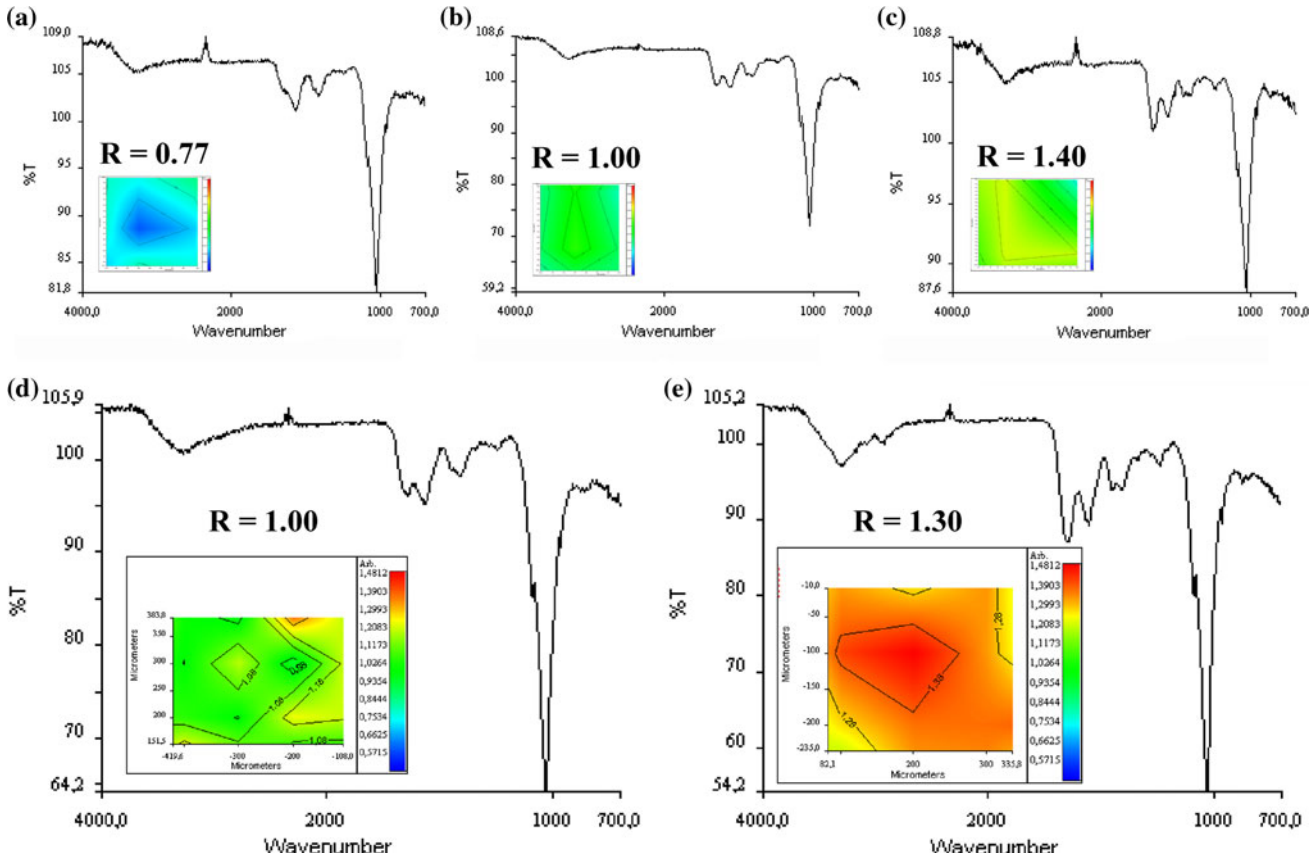

Fig. 7 Transmittance spotlight FT-IR spectra taken in the map areas having the signed amide I to amide II band ratios (R) of a HA_{1100}-Col 80:20 composite (**a**-**c**) and of a CHA-Col 80:20 composite (**d**, **e**)

HA_{1100} ones, it must be taken in account the greater ratios, present in the former, between the amide groups and the phosphate ones, which are only the 83.5% of the whole mineral phase. The fact that the increases are about the same for all the composites examined agrees with this interpretation, although no quantitative calculation can be made, since each area measured is the sum of different absorption bands with different molar absorptivity values, The chemical map (Fig. 6a) of the HA_{1100}-Col 80:20 composite, similar in composition to the natural bone, agrees with the quite uniform distribution of Col and HA in the composite, shown by the correlation map (Fig. 5e). This distribution appears more evident from the amide I to amide II band ratio shown in Fig. 6b. The corresponding maps in Fig. 6c–d confirm that the distribution of the components is substantially uniform also in the composite with 80:20 CHA–Col ratio. The modifications of the spectra in Fig. 7a–c, depending on their positions on the map, are a sign of strong interactions between HA_{1100} and Col; these modifications are near absent from the spectra in Fig. 7d and e. This behaviour indicates that the interactions involving the N–H groups of the peptide bonds and the PO_4^{3-} groups of HA are present more in the composites containing HA_{1100} than in those with CHA. Our findings agree with the studies on the ultra-structure of bone, where the substitution of the phosphate with carbonate was found to cause a decrease of the bone toughness, as greater as the CO_3^{2-} content in the mineral phase of bone is greater [18]. It is likely that, in the presence of CO_3^{2-} ions, the interactions between –N–H and phosphate are diminished, and Ca^{2+} interacts more strongly with the carbonate than with peptide –C=O, so causing a separation between the two components of the bone extra-cellular matrix. This fact is a sign of scarce interactions between CHA and Col, according to the scheme in Fig. 1. The absorbance spectra at different ratios (R) of the amide I absorbance areas to the amide II ones are shown in Fig. 8 for different ratios of both 80:20 composites; the shifts of their maximum absorbance wavenumbers, as well as the variations of the absorbance values, point out the different HA-Col interactions in the two composites, since these bands are sensitive to the structural changes within the Col molecules. One can observe, as R decreases, a shift towards lower wavenumbers of the amide I band at 1643 cm^{-1} and a great decrease of its absorbance, evident in the fibrils containing HA_{1100} (Fig. 8a), because the amide carbonyl stretching is

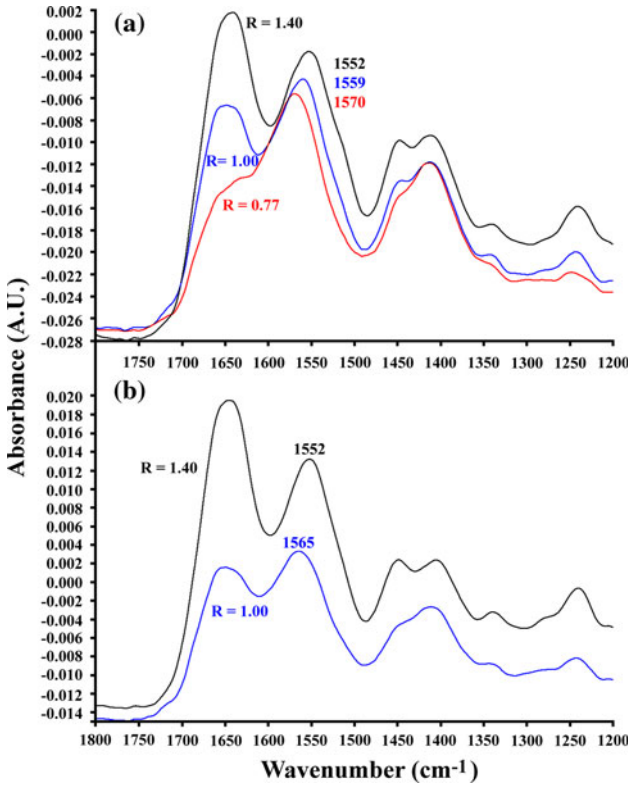

Fig. 8 Absorbance spotlight FT-IR spectra measured in the wave number interval between 1800 and 1200 cm^{-1}, taken at the points having the signed amide I to amide II band ratios (R) in the maps of the HA_{1100}-Col 80:20 composite (**a**) and of the CHA-Col 80:20 composite (**b**)

weakened by the ion–dipole interaction with Ca^{2+}. At the same time a decrease of the intensity of the amide II band occurs, owing to the lower hydration degree due to the substitution of H_2O molecules by HA crystals. Conversely, the same phenomena are less evident in the spectra of the CHA-Col composite shown in Fig. 8b, thus indicating the presence of weaker interactions.

The results obtained could also clarify some physicochemical aspects of the effectiveness of the substances able to bind both Ca^{2+} and Col, like the bisphosphonates and the aminobisphosphonates, as a therapy for osteoporosis [19–22]. However, this mechanism of action cannot explain some negative side effects, like the bone necrosis of the jaws, observed in patients treated with bisphosphonates [23–25]. So, these negative effects, likely correlated with the known interactions of bisphosphonates with osteoclasts and osteoblasts [26], should be studied also from a physicochemical point of view, in addition to the medical and surgical one. An analogous physicochemical study could be useful for the asserted absence of these negative side effects with other anti-osteoporosis drugs, like parathyroid hormone [27, 28], which, however, does not reduce the risk of hip fracture alone [22, 27], and strontium ranelate [29].

Another possible use of these materials is the already proposed fabrication of scaffolds for bone tissue reconstruction [30]; the properties of the composite can be improved, for this purpose, by the chemical or enzymatic covalent cross-linking of the Col fibres [31].

5 Conclusions

In conclusion, the results obtained, although preliminary, show that, in the CHA-Col composite as a synthetic model of the osteoporotic bone, Ca^{2+} interacts more strongly with CO_3^{2-} than with peptide –C=O, so causing a separation between the two components of the bone extra-cellular matrix. This fact strengthens the hypothesis, already proposed [7, 11, 12], of the substitution of PO_4^{3-} ions by CO_3^{2-} ions in the HA lattice as a significant component of osteoporosis. However, more reliable information could be obtained from the mechanical properties of the composites, as well as by making all the tests on ex vivo specimens of both healthy and osteoporotic bone. These researches will be object of future investigation.

Acknowledgments The authors thank Mr. Daniele Marseglia of the Centro di Ricerche ENEA, Brindisi (I), for having carried out the elemental analysis of carbon, and Mr. Piero Narducci of the Dipartimento di Ingegneria Chimica, Chimica Industriale e Scienza dei Materiali, Università di Pisa, for the SEM micrographs of the composites.

References

1. Felsenberg D. Struktur und Funktion des Knochens. Pharm Unserer Zeit. 2001;30:488–94.
2. Marino AA, Becker RO. Evidence for direct physical bonding between the collagen fibres and apatite crystals in bone. Nature. 1967;213:697–8.
3. Thurner PJ, Chen CG, Ionova-Martin S, Sun L, Harman A, Porter A, Ager JW III, Ritchie RO, Alliston T. Osteopontin deficiency increases bone fragility but preserves bone mass. Bone. 2010; 46:1564–73.
4. Walker CG, Dangaria S, Ito Y, Luan X, Diekwisch TGH. Osteopontin is required for unloading-induced osteoclast recruitment and modulation of RANKL expression during tooth drift-associated bone remodeling, but not for super-eruption. Bone. 2010; 47:1020–9.
5. Carrington JL. Aging bone and cartilage: cross-cutting issues. Biochem Biophys Res Commun. 2005;328:700–8.
6. Faibish D, Ott SM, Boskey AL. Mineral changes in osteoporosis. A review. Clin Orthop Relat Res. 2006;443:28–38.
7. Ravaglioli A, Krajewski A. The properties of mineralized natural hydroxyapatite of the bone. In: Ravaglioli A, Krajewski A, Hulbert F, editors. Bioceramics: materials, properties, applications. London: Chapman & Hall; 1992. Appendix B. p. 411–412.
8. Bushinsky DA. Acid-base imbalance and the skeleton. Eur J Nutr. 2001;40:238–44.
9. Stone KL, Seeley DG, Lui L-Y, Cauley JA, Ensrud K, Browner WS, Nevitt MC, Cummings SR. BMD at multiple sites and risk

of fracture of multiple types: long-term results from the study of osteoporotic fractures. J Bone Miner Res. 2003;18:1947–54.
10. Moran P, Towler MR, Chowdhury S, Saunders J, German MJ, Lawson NS, Pollock HM, Pillay I, Lyons D. Preliminary work on the development of a novel detection method for osteoporosis. J Mater Sci Mater Med. 2007;18:969–74.
11. Gagliardi M, Barbani N, Cristallini C, Guerra GD, Krajewski A, Mazzocchi M. Composites between collagen and hydroxyapatite. In: Ravaglioli A, Krajewski A, editors. Proceedings of the 11th meeting and seminar on: ceramics, cells and tissues. Nanotechnology for functional repair and regenerative Medicine, the role of ceramics as in bulk and as coating, Faenza (I) October 2007. Roma: CNR; 2008. p. 182–91. ISBN 88-8080-085-X; 978-88-8080-085-9.
12. Guerra GD. Composites of ceramics and glasses with synthetical and biological macromolecules. In: Ravaglioli A, Krajewski A, editors. Proceedings of the 12th meeting and seminar on: ceramics, cells and tissues. Surface-reactive biomaterials as scaffolds and coatings: interactions with cells and tissues, Faenza (I) May 2009. Roma: CNR; 2009. p. 210–6. ISBN 978-88-8080-111-5.
13. Epstein EH Jr, Scott RD, Miller EJ, Piez HA. Isolation and characterization of the peptides derived from soluble human and baboon skin collagen after cyanogen bromide cleavage. J Biol Chem. 1971;246:1718–24.
14. Krajewski A, Ravaglioli A, Celotti G, Piancastelli A. Characterization and annealing of wet prepared synthetic hydroxyapatite powders for high purity bioceramics. Cryst Res Technol. 1995;30:843–52.
15. Guerra GD, Cerrai P, Tricoli M, Krajewski A, Ravaglioli A, Mazzocchi M, Barbani N. Composites between hydroxyapatite and poly(ε-caprolactone) synthesized in open system at room temperature. J Mater Sci Mater Med. 2006;17:69–79.
16. Itoh S, Kikuchi M, Koyama Y, Takakuda K, Shinomiya K, Tanaka J. Development of a hydroxyapatite/collagen nanocomposite as a medical device. Cell Transpl. 2004;13:451–61.
17. Roveri N, Falini G, Sidoti MC, Tampieri A, Landi E, Sandri M, Parma B. Biologically inspired growth of hydroxyapatite nanocrystals inside self-assembled collagen fibers. Mater Sci Eng C. 2003;23:441–6.
18. Nyman S, Reyes M, Wang X. Effect of ultrastructural changes on the toughness of bone. Micron. 2005;36:566–82.
19. Watts NB. Treatment of osteoporosis with bisphosphonates. Endocrinol Metabol Clin N Am. 1998;27:419–39.
20. McCloskey EV, Beneton M, Charlesworth D, Kayan K, de Takats D, Dey A, Orgee J, Ashford R, Forster M, Cliffe J, Kersh L, Brazier J, Nichol J, Aropuu S, Jalava T, Kanis JA. Clodronate reduces the incidence of fractures in community-dwelling elderly women unselected for osteoporosis: results of a double-blind, placebo-controlled randomized study. J Bone Miner Res. 2007; 22:135–41.
21. Coxon FP, Thompson K, Rogers MJ. Recent advances in understanding the mechanism of action of bisphosphonates. Curr Opin Pharmacol. 2006;6:307–12.
22. Favus MJ. Bisphosphonates for osteoporosis. N Engl J Med. 2010;363:2027–35.
23. Ruggiero SI, Mehrotra B, Rosenberg TJ, Engroff SL. Osteonecrosis of the jaw associated with the use of bisphosphonates: a review of 63 cases. J Oral Maxillofac Surg. 2004;62:527–34.
24. Marx RE, Sawatari Y, Fortin M, Broumand V. Bisphosphonate-induced exposed bone (osteonecrosis/osteopetrosis) of the jaws: risk factors, recognition, prevention, and treatment. J Oral Maxillofac Surg. 2005;63:1567–75.
25. Merigo E, Manfredi M, Meleti M, Guidotti R, Ripasarti A, Zanzucchi E, D'Aleo P, Corradi D, Corcione L, Sesenna E, Ferrari S, Poli T, Bonanini M, Vescovi P. Bone necrosis of the jaws associated with bisphosphonates treatment: a report of twenty-nine cases. Acta Biomed. 2006;77:109–17.
26. Ott SM. Long-term safety of bisphosphonates. J Clin Endocrinol Metab. 2005;90:1897–9.
27. Neer RM, Arnaud CD, Zanchetta JR, Prince R, Gaich GA, Reginster J-Y, Hodsman AB, Eriksen EF, Ish-Shalom S, Genant HK, Wang O, Mitlak BH. Effect of parathyroid hormone (1–34) on fractures and bone mineral density in postmenopausal women with osteoporosis. N Engl J Med. 2001;344:1434–41.
28. Paschalis EP, Glass EV, Donley DW, Eriksen EF. Bone mineral and collagen quality in iliac crest biopsies of patients given teriparatide: new results from the fracture prevention trial. J Clin Endocrinol Metab. 2005;90:4644–9.
29. Reginster JY, Seeman E, De Vernejoul MC, Adami S, Compston J, Phenekos C, Devogelaer JP, Diaz Curiel M, Sawicki A, Goemaere S, Sorensen OH, Felsenberg D, Meunier PJ. Strontium ranelate reduces the risk of nonvertebral fractures in postmenopausal women with osteoporosis: treatment of peripheral osteoporosis (TROPOS) study. J Clin Endocrinol Metab. 2005;90: 2816–22.
30. Bertoni F, Salvucci M, Ciardelli G, Silvestri D, Guerra GD, Giusti P, Barbani N. Hydroxyapatite/collagen interactions: a preliminary study for bone reconstruction nanocomposite scaffolds. In: Proceedings of the 20th European conference on biomaterials, Nantes (F), September 2006, CD-ROM ESB Nantes 2006, Poster file 363.
31. Rosellini E, Barbani N, Cristallini C, Guerra GD. Cross-linked hydroxyapatite-collagen composites as biomaterials for tissue engineering. In: Ravaglioli A, Krajewski A, editors. Proceedings of the 12th meeting and seminar on: ceramics, cells and tissues. Surface-reactive biomaterials as scaffolds and coatings: interactions with cells and tissues, Faenza (I) May 2009. Roma: CNR; 2009. p. 197–204. ISBN 978-88-8080-111-5.